



# CHORUS

This is the accepted manuscript made available via CHORUS. The article has been published as:

## Optical Aharonov-Bohm oscillations in InGaAs quantum wells

L. Schweidenback, T. Ali, A. H. Russ, J. R. Murphy, A. N. Cartwright, A. Petrou, C. H. Li, M. K. Yakes, G. Kioseoglou, B. T. Jonker, and A. Govorov

Phys. Rev. B **85**, 245310 — Published 15 June 2012

DOI: [10.1103/PhysRevB.85.245310](https://doi.org/10.1103/PhysRevB.85.245310)

# Optical Aharonov-Bohm oscillations in InGaAs quantum wells

L. Schweidenback<sup>1</sup>, T. Ali<sup>1</sup>, A.H. Russ<sup>1</sup>, J.R. Murphy<sup>1</sup>, A.N. Cartwright<sup>1</sup>, A. Petrou<sup>1</sup>,  
C.H. Li<sup>2</sup>, M.K. Yakes<sup>2</sup>, G. Kioseoglou<sup>2,4</sup>, B.T. Jonker<sup>2</sup>, A. Govorov<sup>3</sup>

<sup>1</sup>*Department of Physics, University at Buffalo, Buffalo, New York 14260, USA*

<sup>2</sup>*Naval Research Laboratory, Washington, District of Columbia, 20375, USA*

<sup>3</sup>*Department of Physics and Astronomy, Ohio University, Athens, Ohio 45701, USA*

<sup>4</sup>*Department of Materials Science and Technology, University of Crete,*

*Heraklion Crete, 71003, Greece*

## ABSTRACT

The intensity of the photoluminescence emission in InGaAs/GaAs quantum wells (QWs) exhibits local maxima as a function of magnetic field applied perpendicular to the QW plane at low temperatures. These maxima are attributed to the optical Aharonov-Bohm effect associated with spatially indirect excitons that are formed in the vicinity of indium rich InGaAs islands within the QW. Analysis of the data yields the radius of the exciton. The exciton linewidth also oscillates with the magnetic field and exhibits maxima which are shifted slightly to higher field values than those of the luminescence intensity maxima.

The wavefunction of a particle of charge  $q$  that moves on a closed path accumulates the Aharonov-Bohm (AB) phase  $\theta = \frac{q}{\hbar} \Phi$  [1], where  $\Phi$  is the magnetic flux through the closed trajectory and  $\hbar$  is Planck's constant. Manifestations of that phase have been studied using electrical measurements of metallic ring-like nanostructures, in which oscillations of the resistance were observed that are periodic in the magnetic flux penetrating the interior of the ring [2]. The oscillations were attributed to interference between two electron trajectories that traverse the two opposite arms of the ring. The signature of the AB effect has been also detected in the optical properties of negatively charged excitons ( $X^-$ ) in InGaAs/GaAs quantum rings [3]. Oscillations in the energy of the  $X^-$  as function of magnetic field with a period of 1.7 tesla have been observed in this system. This phenomenon is known as the "optical AB effect" (OAB).

It has been predicted theoretically that the OAB effect can also be observed for neutral excitons under certain conditions such as in ring-like nanostructures, where the electron and hole can move over different trajectories resulting in a non-zero dipole moment [4, 5]. Type-II QDs are particularly suitable for observing the OAB effect because of the enhanced polarization of the charged particles resulting from their spatial separation [4, 6]. Experimental verification of this prediction has been provided by several groups. For example, in the InP/GaAs type-II system, where electrons are localized in the InP QDs and the holes orbit in the surrounding GaAs matrix, oscillations in the photoluminescence (PL) intensity with a period of 3.6 tesla have been observed [7]. Another such type-II system is ZnTe/ZnSe in which holes are confined in a ZnTe QD and the electrons move on a closed orbit around the dot in the surrounding ZnSe matrix [8, 9]. The ZnTe/ZnSe system demonstrated OAB-like oscillations in both the intensity and the PL energy [8-10]. One more related study reports observation of OAB oscillations in the energy and the intensity of the PL of a multi-layer type-II Si/Ge QD structure [11]. In the experiments of the above references the type-II band alignment provides favorable conditions for the observation of the OAB-effect, whereas a type-I quantum ring is predicted to have a relatively weak OAB owing to the Coulomb attraction in the exciton [12].

In this work we report the observation of oscillations in the intensity of the PL emitted from InGaAs/GaAs quantum wells which contain indium rich InGaAs islands. The intensity of the excitonic PL exhibits oscillations with magnetic field, superimposed on a monotonically decreasing background. We attribute these oscillations to the OAB effect. We note that the OAB oscillations for neutral excitons in our study appear in InGaAs/GaAs QWs, a material system that is type-I, whereas all previous studies of the OAB effect have been carried out on type-II systems such as InP/GaAs, ZnTe/ZnSe, or Si/Ge. Our observations show that the InGaAs/GaAs system exhibits optical properties of type-II structures due to the presence of indium-rich islands. We have recorded the PL intensity from two undoped 10 nm InGaAs/GaAs single QW structures with indium concentrations 5% (exciton energy = 1.4946 eV) and 15% (exciton energy 1.4315 eV) as a function of magnetic field. The samples were grown by molecular beam epitaxy (MBE) on semi-insulating GaAs(001) substrates. After the growth of undoped GaAs buffer at 580 °C and a brief growth interrupt to optimize surface morphology, the InGaAs was deposited at the same temperature by also opening the shutter to the In Knudsen cell, with a temperature varied between 650 and 685 °C to produce InGaAs QWs with different indium concentrations. A GaAs top cap layer of at least 250 nm was grown immediately after the QW (no growth interrupt) to minimize the indium evaporation. We note that typically InAs (and similarly InGaAs) is grown at lower temperatures (e.g., 450 °C) than GaAs due to the higher evaporation rate of indium. Here we grew InGaAs QWs at the same temperature as GaAs to yield better quality QWs since generally higher quality samples are grown at higher temperatures, at the expense of lower indium concentration. In addition, the fact that the layers are grown at the same temperature also eliminates the growth interrupts needed to stabilize the temperature change.

Cross sectional scanning tunneling microscopy (XSTM) was used to analyze the indium distribution within the InGaAs QWs. For these studies, a reference sample was grown under similar growth conditions on a conductive substrate, and then mounted edgewise and cleaved in ultrahigh vacuum to reveal the cross section of the QW region. Fig.1a shows an atomic resolution XSTM image of the  $\text{In}_{0.15}\text{Ga}_{0.85}\text{As}$  reference QW. The GaAs barriers and InGaAs QW regions are indicated. We note that the large bright

clusters observed randomly throughout the surface are debris likely produced during the cleaving process. Given that Fig.1a is an empty state image, group III atoms (Ga, In) appear as bright, and group V atoms (As) are not visible[13]. For example, each spot in the GaAs barriers represents a Ga atom. Within the InGaAs QW region however, there are also brighter spots that are identified as indium atoms, because their larger size and longer bond length with As cause them to protrude out more from the cleaved surface and therefore appear brighter. Clearly, the indium atoms are not evenly distributed, but rather form small clusters ( $\sim 2\text{-}4$  nm diameter) with a locally higher indium concentration, several of which are indicated by circles. The presence of indium-rich islands has been also suggested in earlier works on InGaAs QWs [14, 15].

We now discuss the conduction and valence band potential profiles in our QWs in the vicinity of the indium rich islands and based on that propose a plausible interpretation of the band-edge emission. A calculation by Pryor[16] shows that the electron potential of a self-organized QD has barriers in the x-y plane at the QD edges as schematically shown in the upper part of Fig.1b. The valence band potential tends to localize the holes at the center of the indium rich island. We note that this potential has no barriers at the QD edges. According to this picture, at low temperatures, the photo-excited electrons do not have enough energy to overcome the conduction band barrier at the edge of the indium-rich islands and therefore remain excluded from the island center. Each electron moves around the island center, held by the Coulomb attraction of the hole as shown in Fig.1b, resulting in a spatially indirect (type-II) exciton indicated by the symbol “X”. Electrons bound to a positively-charged hole inside a two-dimensional QW move in a ring-like orbit around the island. In Fig.1b we also show the spatially direct transition using the symbol “A”.

The continuous wave (cw) luminescence was excited at 785 nm; the emitted light was collected and focused onto the entrance slit of a single monochromator equipped with a cooled CCD multichannel detector. For magnetic field studies the samples were placed in a variable temperature 7 tesla optical magnet cryostat. For the cw reflectance measurements a quasi-monochromatic beam was generated by a combination of a broadband tungsten-halogen source and a single monochromator. The incident beam was

reflected off the sample surface and its intensity was measured as function of the incident photon energy. The time-resolved (TR) luminescence spectra were excited using a pulsed laser system which emits linearly polarized light at a wavelength of 400 nm (repetition rate = 250 kHz, pulse duration  $\sim$ 300 fs). The TR PL was spectrally resolved by a single monochromator, and temporally analyzed by a streak camera (temporal resolution = 40 ps).

The zero magnetic field cw PL and reflectance spectra at  $T = 7$  K from the 5%-indium sample are given in Fig.1c and Fig.1d, respectively. The PL spectrum contains a sharp peak marked “X” at 1494.6 meV and a broader weaker feature centered at 1489.8 meV marked “A”. Corresponding features also appear in the reflectance spectrum. These two spectral features are associated with the transitions marked “X” and “A”, respectively in Fig.1b. The difference in linewidth between feature X and feature A leads us to conclude that X is less sensitive to InGaAs islands ensemble size distribution than feature A. This is probably due to the small mass of the electron, which results in a wide distribution of confinement energies. Feature X in the PL spectrum persists up to 150 K while feature A disappears at 35 K. The temperature sensitivity of feature A excludes the assignment of this feature to a conduction band to acceptor transition since the binding energies of an acceptor in a 100 Å GaAs QW is 30meV[17]. When the temperature is raised, the electron can escape from its shallow conduction band potential well and reside outside the indium-rich island. The large intensity of the excitonic feature in the reflectance spectrum indicates that there is no significant electron population confined in the InGaAs QW [18, 19].

In Fig.2 we plot the intensity of feature X as function of magnetic field  $B$  for the 5% indium sample. Squares indicate data points taken with the magnetic field parallel to the sample normal ( $\varphi = 0$ ). The PL intensity has two maxima at  $B = 2.2$  tesla (labeled “I”) and  $B = 4.4$  tesla (labeled “II”). In contrast, the energy of X does not exhibit oscillations but follows a smooth parabolic dependence on  $B$ . Since we have a negligible electron density in the InGaAs QWs, the oscillations in the PL intensity cannot be attributed to variations in the Fermi energy with magnetic field. Circles in Fig.2 indicate

data points taken with the magnetic field forming an angle  $\varphi = 35^\circ$  with the sample normal. In this case the PL maxima have shifted from 2.2 to 2.6 tesla for feature I, and from 4.4 to 5.5 tesla for feature II, in reasonable agreement with the equation  $B(\varphi) = B(0)/\cos\varphi$ , where B is the magnetic field at the PL maxima. Thus the data of Fig.2 show that the PL intensity oscillations depend on the projection of the magnetic field along the sample normal and vanish altogether when the magnetic field is applied in the sample plane ( $\varphi = 90^\circ$ ). No such oscillations in the PL intensity are present for feature A. In Fig. 3 we plot the PL intensity from the 15% indium sample as a function of magnetic field applied perpendicular to the QW layers. The plot in Fig.3 is similar to that shown in Fig.2 (for the 5% indium) and exhibits maxima at 2.4 and 5.4 T.

We attribute the variations in the PL intensity of the exciton as function of magnetic field to the OAB effect. This effect has been predicted for neutral excitons[4, 6] and has been observed in type-II quantum dots. In our InGaAs/GaAs QW system the OAB effect is associated with spatially indirect excitons that are formed in the vicinity of indium-rich InGaAs islands. Evidence of the presence of these islands was provided by XSTM as has been discussed above. The electrons that are associated with feature X move along a ring-like orbit around the localized hole (see Fig.1b) and, therefore, the exciton is expected to exhibit the optical Aharonov-Bohm effect. This picture is supported by the observation that the PL local intensity maxima in our samples are superimposed on a background that decreases monotonically with increasing magnetic field as shown in Fig.2 and Fig.3. This behavior has been observed in spatially indirect GaAs/AlAs[20] and AlGaAs/AlAs[21] QW structures and has been attributed to spatial localization of the carriers in different regions of the quantum well/barrier interface by the external magnetic field. The interpretation is based on two factors: a) interface defects that can localize electrons and holes on either side of the interface and b) the reduction of the wavefunction size resulting from the external magnetic field. This reduction makes electron and hole localization more efficient and this results in a reduction of the electron-hole wavefunction overlap and a reduction in the PL intensity. In contrast, the PL intensity from spatially direct QWs typically increases with magnetic field [20].

A further indication suggesting the type-II character of feature X in our InGaAs QWs comes from a time-resolved PL comparison between the 5% InGaAs QW and a GaAs reference QW. The PL exciton intensity for both samples is plotted as function of time delay from the exciting laser pulse in Fig.4. The triangle indicates data from the InGaAs QW while the squares denote the results from the reference 10 nm GaAs QW with 250 nm Al<sub>0.14</sub>GaAs barriers grown at 580 °C. The data were fitted with a single exponential which yielded a recombination time of 632 ps for the InGaAs QW (blue line) and 73 ps for the GaAs reference QW (green). The recombination times for the GaAs reference and for the InGaAs QW are in agreement with the results of previous work [15, 22]. We note that Yu et al. attribute the longer times in InGaAs to the presence of indium rich regions [15].

Following the analysis of Kuskovsky et al. [8] the first PL intensity maximum (feature I) in Fig. 2 and Fig.3 is attributed to the energy crossing between the  $L = 0$  and the  $L = -1$  exciton states, where  $L$  is the exciton angular momentum. The second maximum (feature II) is due to the crossing of the  $L = 0$  and the  $L = -2$  exciton states. The corresponding magnetic fluxes  $\Phi_I$  and  $\Phi_{II}$  are equal to  $\Phi_0/2$  and  $\Phi_0$ , respectively [23] where  $\Phi_0 = h/e$  is the flux quantum. If we assume that the exciton wavefunction is circular with radius  $R$ , the magnetic flux through the electron orbit is equal to  $\pi R^2 B$  and a calculation yields a value of 17.3 nm for  $R$  for the 5% sample and 14.8 nm for the 15% sample.

In addition to the PL exciton intensity, the exciton full width at half maximum (FWHM) varies with magnetic field  $B$ . In Fig. 5a we plot the PL intensity (squares) of the exciton of the 5% sample, and its FWHM (circles) as function of  $B$  for  $\varphi = 0$ . Associated with the PL intensity maxima (I) and (II), we observe FWHM maxima (i) and (ii) which occur at magnetic field values that are shifted with respect to the luminescence intensity peaks. A possible interpretation for the positions of the FWHM maxima is given in Fig.5b which is a schematic of the energies of the  $L = 0$  and  $L = -1$  exciton states[8] for feature I. Here we made the assumption that the exciton energies have a finite uncertainty since we deal with an ensemble of localized excitons. As discussed earlier,

the PL maxima occur when the two curves cross (field  $B_2$  in Fig.5b). Field  $B_1$  marks the onset of the crossing of the two exciton states and therefore the increase in PL intensity for feature I. As long as  $E(L = -1)$  is above  $E(L = 0)$ , the former cannot contribute to the exciton linewidth at low temperatures. Once  $E(L = -1)$  moves below  $E(L = 0)$ , starting at  $B_2$ , there is a wider range of allowed exciton energies which results in an increase of the exciton linewidth. Maximum overlap, and therefore maximum in FWHM occurs at field  $B_3$  which is higher than  $B_2$ . For  $B > B_3$ , the energies  $E(L = 0)$  and  $E(L = -1)$  separate and the exciton linewidth is only determined from the width of  $E(L = 0)$ . In our model, the state  $L = 0$  is optically active, whereas the  $L = -1$  state should have a smaller optical dipole moment. Then, because of the thermalization process, at  $B_1$ , most excitons will be at the ground optically-active  $L = 0$  state and the line emission width is expected to become narrower. At  $B_2$ , most of excitons are in the ground  $L = -1$  state, which does not have strong emission, but some excitons still occupy the excited state  $L = 0$  state (according to the Boltzmann exponent,  $\exp[-E/kT]$ ) and give contribution to the PL. Therefore, the PL emission at  $B_3$  comes from two states (from both  $L = -1$  and  $L = 0$  excitons) and can be broader since it involves two states that cannot be resolved. Similar arguments apply for feature II which is due to a crossing of the  $L = 0$  and the  $L = -2$  exciton energies.

We have observed oscillations in the excitonic PL intensity from two InGaAs QWs. These are attributed to the OAB effect associated with spatially indirect excitons which are localized around indium-rich InGaAs islands at low temperatures. The maxima are interpreted as crossings of the  $L = 0$  energy level with the  $L = -1$  and  $L = -2$  states. Analysis of the oscillations yields a value of 17.3 nm for the exciton radius for the 5% indium sample and 14.8 nm for the 15%. Associated with the PL intensity oscillations, we have also observed linewidth oscillations of the exciton PL which have maxima that are slightly shifted to higher magnetic fields as compared to the intensity oscillations.

Acknowledgments: This work was supported by core programs at NRL and by the Office of the Naval Research Contract No. N0001410WX30262. Work at SUNY Buffalo was supported by NSF grant ECCS0824220 and ONR grant N000140910113.

## References:

- [1] Y. Aharonov and D. Bohm, "Significance of Electromagnetic Potentials in the Quantum Theory," *Physical Review*, vol. 115, p. 485, 1959.
- [2] R. A. Webb, S. Washburn, C. P. Umbach, and R. B. Laibowitz, "Observation of H/E Aharonov-Bohm Oscillations in Normal-Metal Rings," *Physical Review Letters*, vol. 54, pp. 2696-2699, 1985.
- [3] M. Bayer, M. Korkusinski, P. Hawrylak, T. Gutbrod, M. Michel, and A. Forchel, "Optical detection of the Aharonov-Bohm effect on a charged particle in a nanoscale quantum ring," *Physical Review Letters*, vol. 90, p. 186801, May 9 2003.
- [4] A. B. Kalameitsev, V. M. Kovalev, and A. O. Govorov, "Magnetoexcitons in type-II quantum dots," *Jetp Letters*, vol. 68, pp. 669-672, Oct 25 1998.
- [5] A. O. Govorov, S. E. Ulloa, K. Karrai, and R. J. Warburton, "Polarized excitons in nanorings and the optical Aharonov-Bohm effect," *Physical Review B*, vol. 66, p. 081309, Aug 15 2002.
- [6] K. L. Janssens, B. Partoens, and F. M. Peeters, "Magnetoexcitons in planar type-II quantum dots in a perpendicular magnetic field," *Physical Review B*, vol. 64, p. 155324, Oct 15 2001.
- [7] E. Ribeiro, A. O. Govorov, W. Carvalho, and G. Medeiros-Ribeiro, "Aharonov-Bohm signature for neutral polarized excitons in type-II quantum dot ensembles," *Physical Review Letters*, vol. 92, p. 126402, Mar 26 2004.
- [8] I. L. Kuskovsky, W. MacDonald, A. O. Govorov, L. Mourokh, X. Wei, M. C. Tamargo, M. Tadic, and F. M. Peeters, "Optical Aharonov-Bohm effect in stacked type-II quantum dots," *Physical Review B*, vol. 76, p. 035342, Jul 2007.
- [9] I. R. Sellers, V. R. Whiteside, I. L. Kuskovsky, A. O. Govorov, and B. D. McCombe, "Aharonov-Bohm excitons at elevated temperatures in type-II ZnTe/ZnSe quantum dots," *Physical Review Letters*, vol. 100, p. 136405, Apr 4 2008.
- [10] I. R. Sellers, A. O. Govorov, and B. D. McCombe, "Optical Aharonov-Bohm Effect in Type-II (ZnMn)Te/ZnSe Quantum Dots," *Journal of Nanoelectronics and Optoelectronics*, vol. 6, pp. 4-19, Mar 2011.
- [11] S. Miyamoto, O. Moutanabbir, T. Ishikawa, M. Eto, E. E. Haller, K. Sawano, Y. Shiraki, and K. M. Itoh, "Excitonic Aharonov-Bohm effect in isotopically pure 70Ge/Si self-assembled type-II quantum dots," *Physical Review B*, vol. 82, p. 073306, Aug 17 2010.
- [12] N. A. J. M. Kleemans, J. H. Blokland, A. G. Taboada, H. C. M. van Genuchten, M. Bozkurt, V. M. Fomin, V. N. Gladilin, D. Granados, J. M. Garcia, P. C. M. Christianen, J. C. Maan, J. T. Devreese, and P. M. Koenraad, "Excitonic behavior in self-assembled InAs/GaAs quantum rings in high magnetic fields," *Physical Review B*, vol. 80, p. 155318, Oct 2009.
- [13] R. M. Feenstra, "Cross-Sectional Scanning-Tunneling-Microscopy of III-V Semiconductor Structures," *Semiconductor Science and Technology*, vol. 9, pp. 2157-2168, Dec 1994.

- [14] H. P. Yu, C. Roberts, and R. Murray, "Influence of Indium Segregation on the Emission from InGaAs/GaAs Quantum-Wells," *Applied Physics Letters*, vol. 66, pp. 2253-2255, Apr 24 1995.
- [15] H. P. Yu, C. Roberts, and R. Murray, "Exciton Recombination Dynamics in  $\text{In}_x\text{Ga}_{1-x}\text{As}/\text{GaAs}$  Quantum-Wells," *Physical Review B*, vol. 52, pp. 1493-1496, Jul 15 1995.
- [16] C. Pryor, "Eight-band calculations of strained InAs/GaAs quantum dots compared with one-, four-, and six-band approximations," *Physical Review B*, vol. 57, pp. 7190-7195, Mar 15 1998.
- [17] R. C. Miller, A. C. Gossard, W. T. Tsang, and O. Munteanu, "Extrinsic Photo-Luminescence from GaAs Quantum Wells," *Physical Review B*, vol. 25, pp. 3871-3877, 1982.
- [18] A. Ruckenstein and S. Schmitt-Rink, *Physical Review B*, vol. 35, p. 7551, 1987.
- [19] J. P. Loehr and J. Singh, "Nonvariational Numerical-Calculations of Excitonic Properties in Quantum-Wells in the Presence of Strain, Electric-Fields, and Free-Carriers," *Physical Review B*, vol. 42, pp. 7154-7162, Oct 15 1990.
- [20] A. Truby, M. Potemski, and R. Planel, "Magnetic field effects in the luminescence spectra of type II GaAs/AlAs double layer structures," *Solid-State Electronics*, vol. 40, pp. 139-141, 1996.
- [21] J. Haetty, M. Salib, A. Petrou, T. Schmiedel, M. Dutta, J. Pamulapati, P. G. Newman, and K. K. Bajaj, "Magnetic-field-induced localization of carriers in  $\text{Al}_{0.25}\text{Ga}_{0.75}\text{As}/\text{AlAs}$  multiple-quantum-well structures," *Physical Review B*, vol. 56, pp. 12364-12368, Nov 15 1997.
- [22] G. Finkelstein, V. Umansky, I. Bar-Joseph, V. Ciulin, S. Haacke, J. D. Ganiere, and B. Deveaud, "Charged exciton dynamics in GaAs quantum wells," *Physical Review B*, vol. 58, pp. 12637-12640, Nov 15 1998.
- [23] L. G. G. V. D. da Silva, S. E. Ulloa, and A. O. Govorov, "Impurity effects on the Aharonov-Bohm optical signatures of neutral quantum-ring magnetoexcitons," *Physical Review B*, vol. 70, p. 155318, Oct 2004.

## Figure Captions

Fig.1: (Color online) (a) Cross-sectional scanning tunneling microscopy image of a similarly grown InGaAs QW on a conductive substrate. Sample bias = 2 V, tunneling current = 0.06 nA. The straight lines mark the GaAs/InGaAs interfaces; the circles indicate indium rich islands. (b) Schematic of the conduction and valence band edges in the vicinity of an indium rich island [16] and schematic of the spatially indirect exciton associated with indium rich islands. The hole is confined at the center of the island, while the electron is held outside by the electron-hole Coulomb attraction. (c) PL spectrum from the 5% InGaAs QW at  $T = 7$  K (d) Reflectance spectrum from the 5% InGaAs QW at  $T = 7$  K

Fig.2: (Color online) Intensity of the excitonic feature plotted as function of magnetic field for the 5% InGaAs QW at  $T = 7$  K. (a): Magnetic field parallel to the sample normal (b) Magnetic field at an angle  $\phi = 35^\circ$  with the sample normal.

Fig.3: (Color online) Intensity of the excitonic feature plotted as function of magnetic field for the 15% InGaAs QW at  $T = 7$  K with the magnetic field parallel to the sample normal.

Fig.4: (Color online) Intensity of the exciton PL as function of time-delay between the exciting laser pulse and detection for a 10 nm GaAs/AlGaAs QW and 10 nm 5% InGaAs QW. The solid lines represent fits to the data with a single exponential.

Fig.5: (Color online) (a): Plot of the exciton PL intensity (squares) and the exciton FWHM (circles) as a function of magnetic field applied along the z-axis ( $\phi = 0$ ); (b): Schematic diagram of the energies of the  $L = 0$  and  $L = -1$  exciton states in the vicinity of their crossing.

Fig 1a

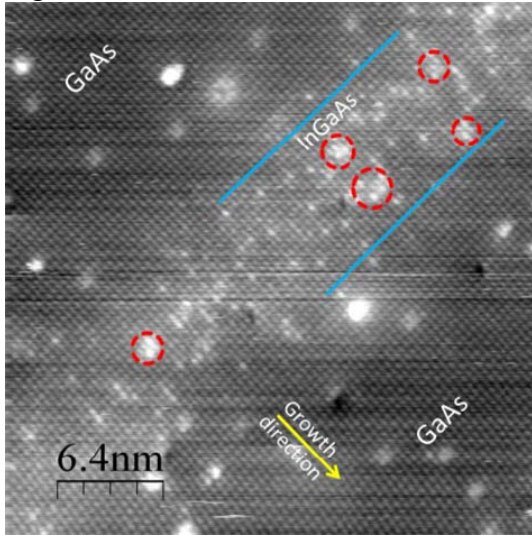


Fig 1b

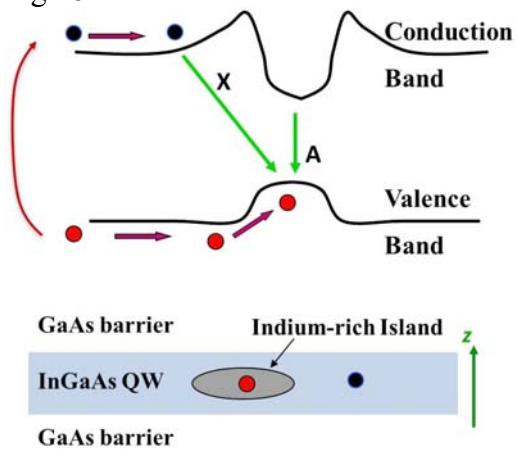


Fig 1c&d

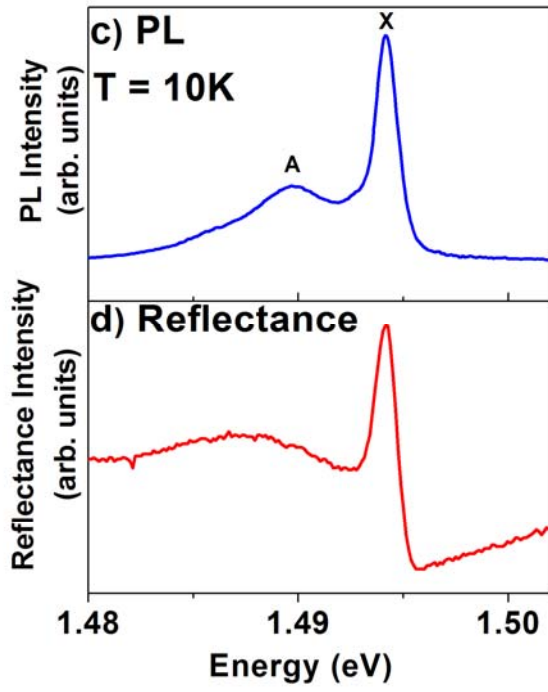


Fig 2

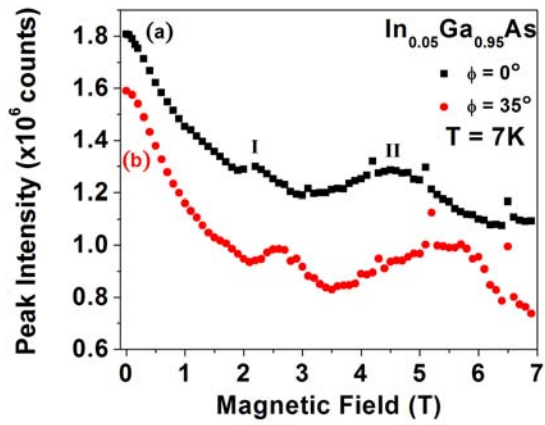


Fig 3

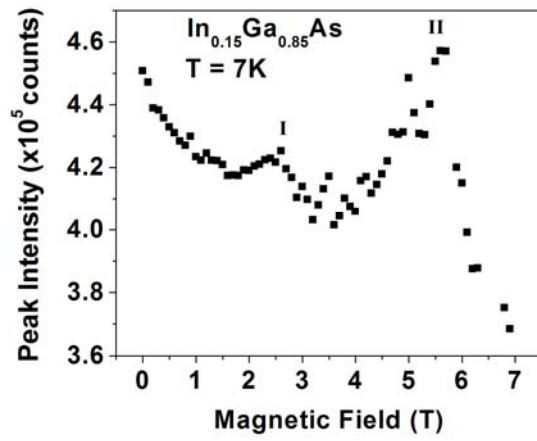


Fig 4

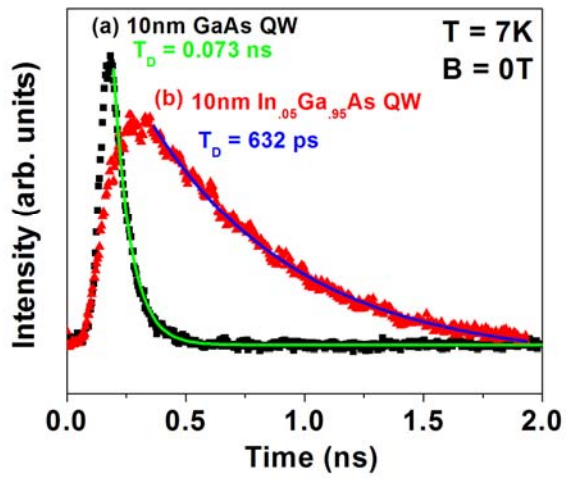


Fig5

